STEADY-STATE PERFORMANCE OF A CONTINUOUS BIOFILM FERMENTOR SYSTEM FOR PENICILLIN PRODUCTION

Young H. Park and D.A. Wallis***

Division of Biological Science and Engineering, Korea Advanced Institute of Science and Technology, Seoul, Korea

* Department of Chemical Engineering, Virginia Polytechnic Institute and State University, Blacksburg, VA 24061, U.S.A.

(Received 21 April 1984 • accepted 23 May 1984)

Abstract—Steady-state performance of a three-phase fluidized-bed biofilm fermentor system, which is used for production of penicillin, is analyzed by considering two ideal contacting patterns, i.e., complete-mixed and plug-flow ones. At steady state, the biofilm thickness is kept constant by assuming that the microbial growth is balanced with cell decay processes. From the simulation analyses, it was found that a complete-mixed contacting pattern gives superior performance to plug-flow one in both outlet product concentration and specific productivity of the reactor system. The inhibitory effect of the carbon source, glucose, is found to be less pronounced in the former configuration, and this fact is considered an important criterion for the design purposes. Optimum biofilm thickness for the biofilm fermentor system was found to be a function of various operating parameters such as inlet substrate concentration and oxygen transfer capacity of the system. It should therefore not be determined directly from the penetration depth of a limiting nutrient, but from information on the interactions between reactor productivity and those operating variables.

INTRODUCTION

Recently, immobilization of living microorganisms and its use in fermentation systems are of increasing interests in biotechnology research field. In the biofilm fermentor system, microorganism is immobilized on inert solid particles and forms microbial film layer on the surface of the carrier. Traditionally, such biofilm reactors have been extensively used in waste-treatment processes, [1,2] mainly because of their relatively cheap cost of operation. However, as indicated by Atkinson [3] and Atkinson et al. [4,5], this type of bioreactor can also be applied to more complex fermentation systems for primary and secondary metabolites, even though such applications are as yet quite rare. The use of biofilm reactors for such purposes may possess several advantages over conventional reactors like batch or fed-batch type fermentors [4,5]: (1) higher productivity due to the greater biomass hold-up, (2) extended production phase by continuous supply of substrates, precursors and/or inducers, (3) high oxygen transfer rate due to the low liquid phase viscosity, (4) ease of biomass recovery, (5) possibilities of a wider range of reactor configurations, (6) use of preferred characteristic size of bioparticles for improved reactor productivity, and (7) lower power consumption.

A fixed-bed type biofilm fermentor was recently tested for citric acid production [6] and was reported to have a lower product yield than a regular batch type stirred fermentor, mainly because of severe oxygen limitation.

This situation could be corrected by using a fluidized-bed type biofilm fermentor in which bioparticles are fluidized by both liquid growth medium and air. This should result in a higher oxygen transfer rate due to sufficient turbulence in the liquid phase. However, an appropriate mathematical modelling and simulation study is required in advance for proper design and analysis of such three phase microbial fermentor systems. This theoretical work must involve the effects of mass transfer across the biofilm layer and co-utilization of the limiting substrate and oxygen. The principal purpose of this study is to explore the feasibility of using biofilm fermentor systems for the production of microbial secondary metabolites. Penicillin has been chosen as a model system since relatively sufficient

** To whom correspondence should be directed.

kinetic information is available. In this article, the effects of biofilm thickness and contacting patterns on the system productivity are analyzed through a computer simulation technique using appropriate mathematical models.

THEORETICAL DEVELOPMENT

2.1. Reaction Kinetics

Several kinetic models have been suggested for the penicillin fermentation system; a model based on logistic law used by Constantinides et al. [7] a cell age model by Calam and Ismail [8], a model using an elemental balancing method by Heijnen et al.,[9] and enzyme kinetic models by Fisherman and Biryukov, [10] and Bajpai and Reuss [11]. However, only the model by Bajpai and Reuss considers the oxygen demand for cell growth and product formation during the fermentation process. According to Ryu [12] and Giona et al. [13], the rate of penicillin production is greatly reduced by a limitation of oxygen transfer in the bulk phase. This oxygen limitation effect on penicillin fermentation has been analyzed by Bajpai and Reuss [14]. It is likely that in a biofilm fermentor, diffusion of oxygen into the biofilm layer becomes a controlling step for the product formation. Therefore the model suggested by Bajpai and Reuss [11], which contains the effects of both carbon substrate and oxygen, was chosen to be used in this study. In the model, the rates of cell growth and product formation, Rx and Rp, respectively, are expressed as,

$$Rx = \frac{dX}{dt} = Ux \frac{S}{KxX + S} \frac{Co}{KoxX + Co} X \quad (1)$$

$$Rp = \frac{dp}{dt} = Up \frac{S}{Kp + S(1 + S/Ki)} \frac{Co_X}{KopX + Co} \quad (2)$$

It can be noted that the rate equations (1) and (2) involve double Contois kinetic model with respect to the substrate and oxygen concentrations. In the eq. (2), the effect of catabolite inhibition of readily utilizable carbon source on product formation is considered by employing substrate inhibition kinetics. Then the consumption rates of substrate and dissolved oxygen, R_s and R_{o2}, respectively, are expressed as,

$$R_s = -\frac{dS}{dt} = \frac{1}{Y_{x/s}} R_x + \frac{1}{Y_{p/s}} R_p - m_s X \quad (3)$$

$$R_{o2} = -\frac{dCo}{dt} = \frac{1}{Y_{x/o}} R_x + \frac{1}{Y_{p/o}} R_p + m_o X \quad (4)$$

The values of kinetic parameters for the equations (1) through (4), suggested by Bajpai and Reuss [11], are listed in Table 1. Note that the equation for biomass growth, eq. (1), takes a form of double Monod model when cell mass density in the biofilm layer, X, is assumed constant.

Table 1. Kinetic Parameters used in this study [11].

Parameter	Value	Units
U_x	0.1	(hr^{-1})
U_p	4×10^{-3}	(mg penicillin/mg drycell/hr)
K_x	6×10^{-3}	(mg substrate/mg dry cell)
K_p	2×10^{-4}	(mg/cm^3)
K_i	0.1	(mg/cm^3)
K_{ox}	$1.11 \times 10^{-3} Co^*$ +	(μmole O_2/mg dry cell)
m_s	0.014	(mg substrate/mg dry cell/hr)
m_o	0.467	μmole O_2/mg dry cell/hr)
$Y_{x/s}$	0.45	(mg dry cell/mg substrate)
$Y_{x/o}$	0.04	(mg dry cell/μmole O_2)
$Y_{p/s}$	1.2	(mg penicillin/mg substrate)
$Y_{p/o}$	0.2	(mg penicillin/μmole O_2

+ solubility of oxygen in liquid substrate, Co*, set at 1.26 μ.mole $0_2/cm^3$.

2.2. Reactor Kinetics

For aerobic fermentations, the system involves three phases, viz., liquid (substrate solution), solid (cell mass) and gas (air) phases. In a biofilm fermentor system, the solid phase consists of solid particles which are coated with a microbial slime layer (bioparticle, Fig. 1). Since oxygen mass transfer can be a rate limiting step in such a system [4,6], a fluidized-bed arrangement is preferred to a fixed-bed type operation, because the oxygen transfer rate can be significantly increased by turbulence in the liquid phase [15], To analyze such a three-phase fluidized-bed system, two ideal contacting patterns, complete-mixed and plug-flow, are considered in this work. Actual performance of the three-phase fluidized-bed reactor system is expected to fall in between those for the complete-mixed and plug-flow arrangements. Attaining a steady-state condition is important for stable and long-term operation of such a continuous reactor system. Here, the term "steady-state" implies that the biofilm thickness is constant due to a balance between microbial growth and cell decay processes, as suggested by Rittmann [16] and Andrews [17]. Cell decay is considered to include sloughing-off of cell mass from the solid support due to the shear force in the culture broth, and cell lysis due to the nutrient starvation inside the biofilm. In addition to this definition of steady-state condition, following assumptions are made for bioparticles:

1) each bioparticle is spherical, with the radii of inert solid support and the support with attached microbial film layer (see Fig. 1), R_o and R_f, respectively.

2) the properties of the biofilm layer, including density, cell concentration and diffusivities, do not vary with radial direction.
3) the diffusional resistance of the liquid film outside the bioparticle is negligible.

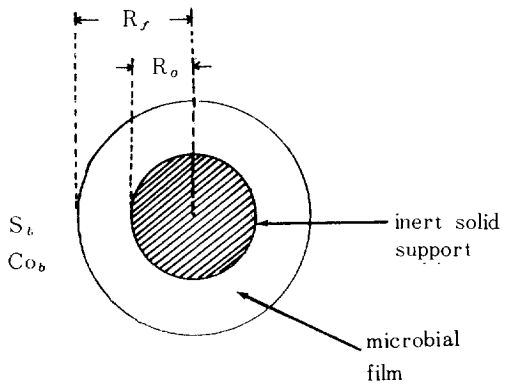

Fig. 1. A schematic diagram of a spherical bioparticle with attached biofilm layer.

In practice, the second assumption may not strictly be true, because inside the biofilm the microbial metabolism may be limited by low substrate and/or oxygen concentrations which are different from the surface of the bioparticle. However, one must assume constant conditions since no quantitative information is available on such property changes within the biofilm. The third assumption is considered reasonable because the external mass transfer resistance becomes negligible for relatively high through-puts which is needed for proper expansion of the bed [18]. It is also justified by high Biot number ($Bi = k_l Rf/D^e$: where k_l is mass transfer coefficient, and D^e the effective diffusivity of the substance molecule) in the external boundary layer. For glucose and oxygen, the values of Biot numbers are in the range of 10^2—10^3, which are high enough to neglect the mass transfer resistance in the boundary layer [19]. Using these assumptions and the rates of substrate and oxygen utilization defined by the Eqs. (3) and (4), the following transport equations can be derived from steady-state material balances over the differential volume of biofilm.

Substrate

$$D_S \frac{1}{r^2}\frac{d}{dr}\left(r^2\frac{dS}{dr}\right) = \frac{1}{Y_{X/S}}R_X + \frac{1}{Y_{P/S}}R_P + m_S X \quad (5)$$

Dissolved Oxygen

$$Do\frac{1}{r^2}\frac{d}{dr}\left(r^2\frac{dCo}{dr}\right) = \frac{1}{Y_{X/O}}R_X + \frac{1}{Y_{P/O}}R_P + m_O X \quad (6)$$

Where Ds and Do are the effective diffusivities of the substrate and oxygen within the biofilm phase. The boundary conditions associated with these differential equations are,

$$\left.\begin{aligned}\frac{dS}{dr} &= 0 \quad (7)\\ \frac{dCo}{dr} &= 0 \quad (8)\end{aligned}\right\} \quad \text{at } r = Ro,$$

$$\left.\begin{aligned}S &= Sb \quad (9)\\ Co &= Cob \quad (10)\end{aligned}\right\} \quad \text{at } r = R_f,$$

The conditions (7) and (8) imply that the fluxes of substrate and oxygen are zero at the surface of inert solid particle, since no reaction occurs in the support material. The condition of negligible external mass transfer resistance around the biofilm is reflected in Eqs. (9) and (10). It should be noted that the "zero-flux" condition (Eqs. (7) and (8)) is applicable only to the case for which the nutrients are not deficient inside the biofilm.

When the concentrations of substrate or oxygen fall to zero inside the biofilm (nutrient-deficient cases), the boundary conditions (7) and (8) should be replaced by,

$$\frac{dS}{dr} = 0 \qquad \text{at } r = r_{cs}, \quad (7')$$

$$\frac{dCo}{dr} = 0 \qquad \text{at } r = r_{co}, \quad (8')$$

Where r_{cs} and r_{co} are the radial positions within the biofilm at which the substrate and oxygen become deficient. These boundary conditions are employed since there will be no biomass growth, substrate utilization, or product formation in the portion of the biofilm where such deficiencies occur. Bulk concentrations of substrate and dssolved oxygen, S_b and Co_b, respectively, are to be evaluated from the reactor dynamics for corresponding contacting patterns and their operating conditions.

2.3. Complete-mixed contacting pattern

For a complete-mixed contacting pattern, following assumptions are made:

1) Gas and liquid phases are completely mixed. This implies that pH, temperature, and the concentrations of substrate, dissolved oxygen and product in the liquid phase are uniform throughout the fermentor.
2) Bioparticles are evenly distributed in the reactor, and the size of bioparticle is uniform.
3) Substrate feed stream is presaturated with oxygen.
4) Oxygen uptake is taken place only in the liquid phase, i.e., direct uptake from the gas phase is negligible.

With these assumptions, the steady state material balance equation for the substrate yields,

$$Q(S_o - S_b) - V \cdot R_s = 0, \quad (11)$$

The overall substrate consumption rate, $V \cdot R_s$, is expressed as,

$$V \cdot R_s = \frac{V(1-\varepsilon)}{4/3\pi R_f^3} \; 4\pi R_f^2 \, Ds \frac{ds}{dr}\Big|_{r=R_f} \tag{12}$$

Substituting Eq. (12) into Eq. (11), the bulk substrate concentration is given by,

$$S_b = S_o \cdot (1 - K_s \cdot \theta \cdot N_s) \tag{13}$$

Where $K_s = 3(1-\varepsilon)\; D_s/(1+\delta)\; R_o^2$,

$\theta = \frac{V}{Q}$ = mean residence time (hr),

$N_s = \frac{R_o}{S_o} \frac{ds}{dr}\Big|_{r=R_f}$,

Similarly, the bulk concentration of dissolved oxygen is given by,

$$Co_b = Co^* \cdot \left[1 - \frac{\theta}{(1+\theta \cdot k_l a)} K_o \cdot N_o\right] \tag{14}$$

Where $Ko = 3(1-\varepsilon) \cdot Do/(1+\delta)\; Ro^2$,

$No = \frac{Ro}{Co^*} \frac{dCo}{dr}\Big|_{r=R_f}$,

k_l = liquid side mass transfer coefficient between air bubble and bulk liquid (cm/hr),

a = effective oxygen mass transfer area per unit volume of liquid (cm^{-1}),

Co^* = solubility of oxygen in liquid substrate (μmole O_2/cm^3).

The concentration profiles of substrate and oxygen inside the biofilm are now determined by solving the systen of ordinary differential equations consisted of Eqs. (5) through (14). Once the concentration profiles are calculated, the product concentration in the bulk phase can be evaluated. The steadystate material balance equation on product is given by,

$$Q(p_{in} - P_b) + V \cdot R_p = o \tag{15}$$

The overall product formation rate, $V \cdot R_p$, is defined by,

$$V \cdot R_p = N_p V_f \left[\frac{1}{V_f} \int_{R_o}^{R_f} 4\pi r^2 \frac{Up \cdot S \cdot X}{Kp + S(1+S/Ki)} \frac{Co}{KopX + Co} dr\right] \tag{16}$$

where Np = total number of bioparticles in the fermentor
$= V(1-\varepsilon)/(4/3\,\pi R_f^3)$,

V_f = volume of biofilm layer on an individual bioparticle
$= 4/3\pi(R_f^3 - R_o^3)$

Note that the value of the bracket in Eq. (16) is the volume average product formation rate for individual bioparticles at steady state. With no product in the feed stream, i.e., Pin = o, the product concentration in the outlet stream is given by,

$$P_b = \theta \frac{3(1-\varepsilon)}{(1+\delta)^2} Up X \int_1^{1+\delta} \xi^2 \frac{S}{K_p + S(1+S/K_i)} \frac{Co}{K_{op}X + Co} d\xi \tag{17}$$

2.4. Plug-flow Contacting Pattern

In deriving the plug-flow reactor model, the same assumptions are applied as for the CSTR, except that the liquid and gas phases are in plug-flow mode. Additional assumptions for the plug-flow model are;

1) The volume fraction occupied by gas phase, Φ, is constant over the entire reactor length.
2) The liquid phase oxygen mass transfer coefficient, $k_l a$, is constant through out the total reactor length.

These assumptions are used because most available experimental results obtained from bubble columns or three phase fluidized beds show a negligible effect of column height on the air hold-up and $k_l a$ except for very tall columns [15,20,21].

Using these assumptions, the steady-state mass balances for substrate and dissolved oxygen yield,

Substrate in liquid phase

$$u_l(1-\Phi)\frac{dS_b}{dz} + (1-\Phi)\frac{3(1-\varepsilon)}{R_f} Ds \frac{dS}{dr}\Big|_{r=R_f} = 0 \tag{18}$$

Dissolved oxygen in liquid phase

$$u_l(1-\Phi)\frac{dCo_b}{dz} + (1-\Phi)\frac{3(1-\varepsilon)}{R_f} Do \frac{dCo}{dr}\Big|_{r=R_f} = 0 \tag{19}$$

Oxygen in gas phase

$$u_g \frac{\Phi}{RT}\frac{dP_{o_2}}{dz} + k_l a(P_{o_2}/H - Co_b) = 0 \tag{20}$$

The first and second terms of Eqs. (18) and (19) represent the change by convection and the rate of disappearance of the substrate and oxygen in the differential height of the reactor, dz, respectively. In Eq. (20), Φ is the volume fraction occupied by the gas phase in the total bed volume, P_{o2} the partial pressure of oxygen, H the Henry's law constant for oxygen. The terms u_l and u_g are the superficial velocities of liquid and gas, respectively.

It is known that a plug-flow model is theoretically equivalent to a CSTR (continuous stirred rank reactor) arrangement with infinite number of stages in series. In other words, plug-flow behavior can be adequately

simulated by employing a series of CSTR's for which the total volume is the same as the original plug-flow reactor. In this study, fifty equal-sized CSTR's are used to approximate the plug-flow performance, which were found most adequate to describe the system of present investigation [22].

NUMERICAL TECHNIQUE

A computation software package, COLSYS [23], is used to solve the boundary value problem described in the previous section. B-spline collocation method [24] is employed in the package COLSYS to solve this type of boundary value problem and has been found to be the most efficient technique for this kind of study. The major advantage of using COLSYS is that it uses a formerly obtained approximate solution as a first approximation for a non-linear iteration on a new problem (e.g., for continuation purposes). In this study, this continuation technique of COLSYS is most useful, especially for the multistage CSTR approximation of the plug-flow model.

RESULTS AND DISCUSSION

4.1. Steady-state Biofilm Kinetics

Fig. 2 demonstrates typcal profiles of substrate and oxygen concentration through a biofilm of 0.02 cm thickness when the radius of inert carrier is 0.05 cm (dimensionless biofilm thickness, δ = 0.4). These results are based on a complete-mixed contacting pattern and a residence time of 1 hr.. At an inlet substrate concentration, So, of 20 g glucose/liter, the substrate concentration decreases from about 18.5 g/liter at the outer film surface to about 18.2 g/l at the solid support-microbial film interface. At this high concentration, the oxygen concentration decreases rapidly to zero such that a significant portion of biofilm is under the conditions of severe oxygen limitation. Thus the average rate of product formation is limited by the lack of a sufficient supply of oxygen. It should also be noted, however, in this case that even with adequate oxygen supply, the product formation would be relatively slow due to the inhibition by high substrate concentration inside the biofilm. A similar but less drastic situation exists for the case of So=2 g/l, although oxygen limitation is not as severe. For So=1g/l, oxygen concentration appears to remain high enough throughout the biofilm layer for the oxygen supply to be adequate.

It has been proposed[3,4,5] that the penetration depth of a limiting nutrient be used to define the "ideal film thickness". Based on this idea, an inlet concentration between 1 and 2 g/l would be optimum for this biofilm thickness. However, it is obvious from Fig. 3 that this is not a true case, and So=0.5g/l will yield higher

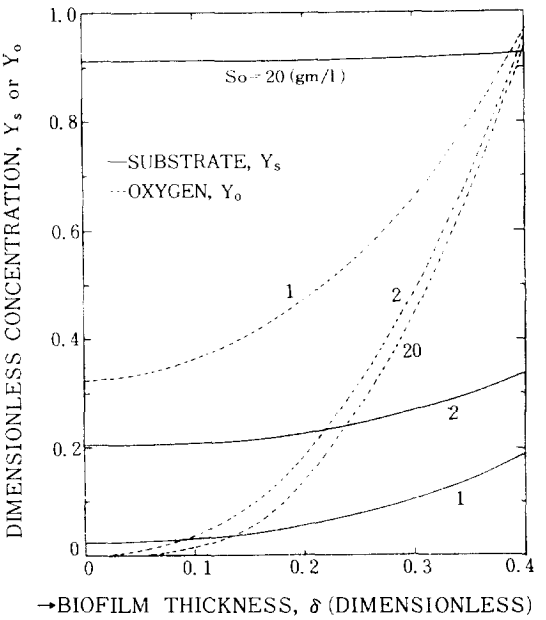

Fig. 2. Dimensionless concentration profiles of the substrate(—) and oxygen(···) in the subfilm layer δ=0.4 and θ=1hr. The numbers for each curve indicate the initial substrate concentration, S_o(g Glucose/liter).

product concentration (at the dimensionless biofilm thickness, =0.4) and thus higher specific productivity. This is because that the substrate inhibition effect on product synthesis is less pronounced for lower values of S_o. As shown in Figs. 3 and 4, thicker biofilm yields higher outlet product concentration and specific productivity unless product formation becomes limited by substrate and/or oxygen deficiency inside the biofilm layer. This indicates that there exists an "optimum" biofilm thickness for a given inlet substrate concentration, which is obviously different from the penetration depth of a limiting nutrient as defined elesewhere. It can also be noted from Figs. 3 and 4 that the optimum film thickness for a given inlet substrate concentration, or vice versa, is a function on the contacting pattern in the reactor. In addition, it is interesting to note that the optimum biofilm thickness for So=0.5 g/l is roughly the same as that for So=2 g/l (complete-mixing case). The production rate for the latter case is, however, much lower due to the substrate inhibition effect.

4.2. Analysis of complete-mixed reactor

Fig. 5 and 6 show typical profiles of outlet product concentrations and specific productivities for various inlet substrate concentrations (g glucose/liter) at varying mean residence times (hours). The steady-state biofilm thickness, is 0.3 (dimensionless). It is noted from Fig. 5

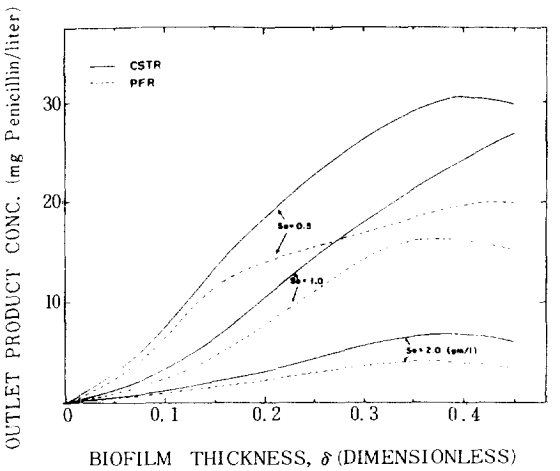

Fig. 3. Effect of biofilm thickness on product concentration in the outlet streams of two contacting patterns, $\theta = 1$hr.

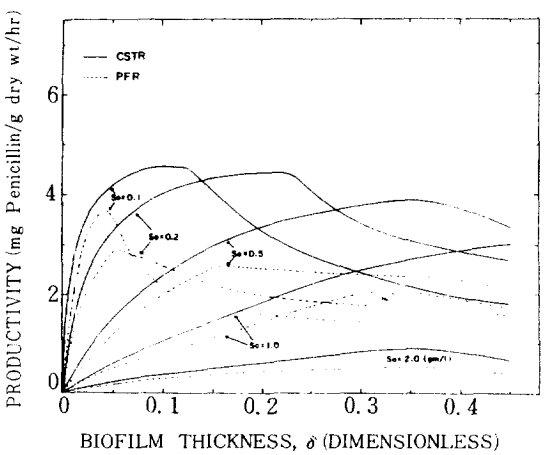

Fig. 4. Effect of biofilm thickness on the specific productivity of the contacting patterns, $\theta = 1$hr.

that increasing inlet substrate concentration yields increased final product concentration, but requires longer residence time. The initial increase in product concentration can be explained by the effect of substrate inhibition.

This is because of the fact that steady-state bulk substrate concentration, S_b, decreases as mean residence time increases. It is interesting to note from Fig. 6 that the maximum attainable productivity is constant for all inlet substrate concentrations at a fixed biofilm thickness. This was expected in light of the model used for the specific production rate of penicillin, which is a function of substrate and oxygen concentration only. The oxygen concentration profile through a

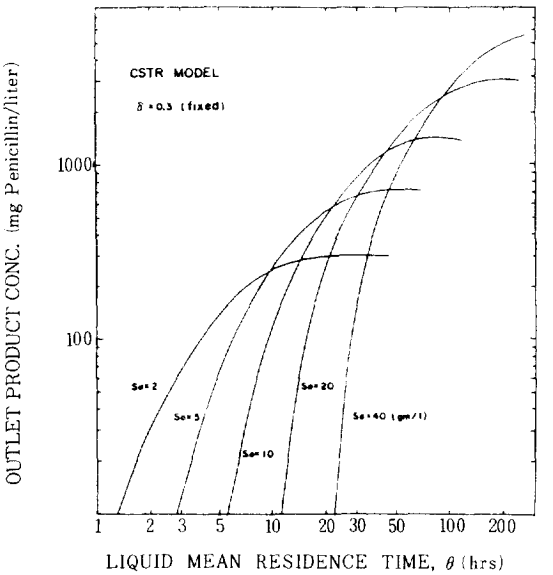

Fig. 5. Product concentrations in the outlet stream for a CSTR contacting pattern at various space times, $\delta = 0.3$.

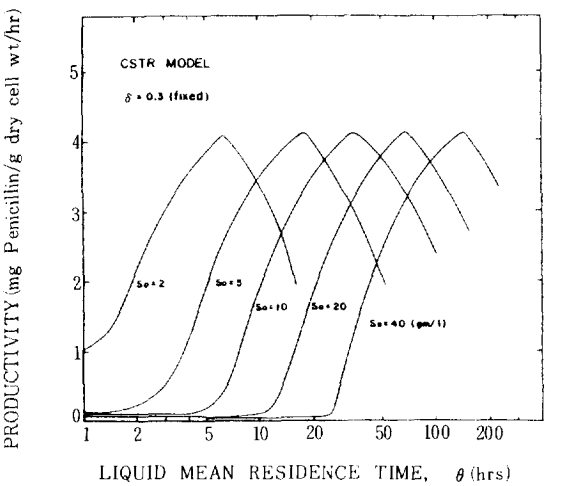

Fig. 6. Specific pro ductivities of a CSTR contacting pattern at various space times, $\delta = 0.3$.

biofilm layer was, as shown previously (Fig. 2), a function of substrate concentration employed, for a fixed biofilm thickness. Therefore, there exists a bulk substrate concentration most favorable for product formation. An increase in S_0 requires longer residence time to maintain optimum levels of S_b and oxygen concentration. The effects of oxygen concentration can be demonstrated by increasing biofilm thickness. As shown in Table 2, the maximum attainable productivity

decreases as the biofilm thickness is increased. This is because a larger fraction of the cell mass in the biofilm is oxygen limited for thicker biofilms, even under the conditions at which the bulk substrate concentration is most favorable for product formation. Thus the efficiency of the cell mass for product formation is greater for thinner biofilm (high productivity). But it should also be noted that, for a given number of bioparticles in the fermentor, a thicker biofilm and higher inlet substrate concentration are required to achieve high outlet product concentration.

Table 2. Maximum attainable productivity in CSTR, $S_0 = 10$ (g/liter).

Dimensionless Biofilm Thickness	Maximum Productivity*	Residence Time(hrs)
0.10	4.38	90
0.15	4.45	75
0.20	4.39	60
0.25	4.26	47
0.30	4.11	35
0.35	3.95	31

* Unit is (mg penicillin/g dry cell weight/hr).

4.3. Analysis of plug-flow reactor

The effects of increasing inlet substrate concentration on final product concentration and specific productivity for a plug flow reactor are much different from those of the complete-mixed system. As noted from Fig. 7, the maximum outlet product concentration increases only by a factor of about three for an increase in inlet substrate concentration from 2 to 40 g glucose/liter. By definition, bulk substrate concentration in a plug flow reactor decreases as the substrate flow moves toward the reactor outlet.

Therefore, at high inlet concentrations, a significant portion of the reactor toward the inlet is under conditions of severe substrate inhibition for product synthesis. Similarly, a significant portion of the reactor toward the outlet suffers from substrate deficiency. This means that in a plug-flow configuration, only a very small portion of biomass in the reactor is active for product formation. Thus, the slight increase in product concentration that does result from an increase in inlet substrate concentration is explained by a change in bulk substrate concentration profile along the reactor, such that product formation occurs at a faster specific rate. This implies that a larger fraction of the substrate is used for product synthesis, and less is consumed for cell growth and maintenance purposes.

Fig. 8 shows a decrease in maximum attainable specific productivity as the substrate concentration in-

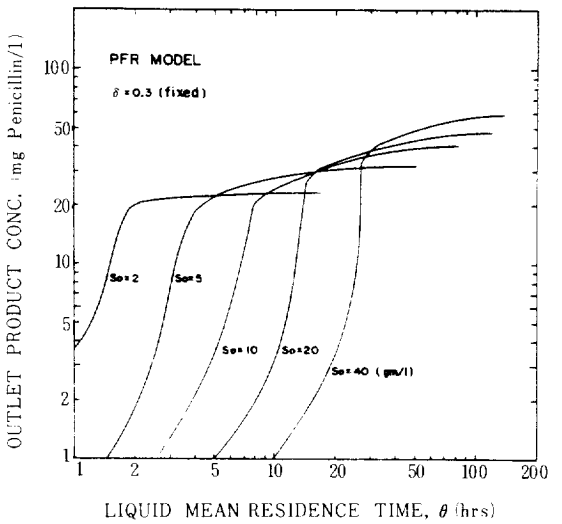

Fig. 7. Product concentrations in the outlet stream for a PFR contacting pattern at various space times, $\delta = 0.3$.

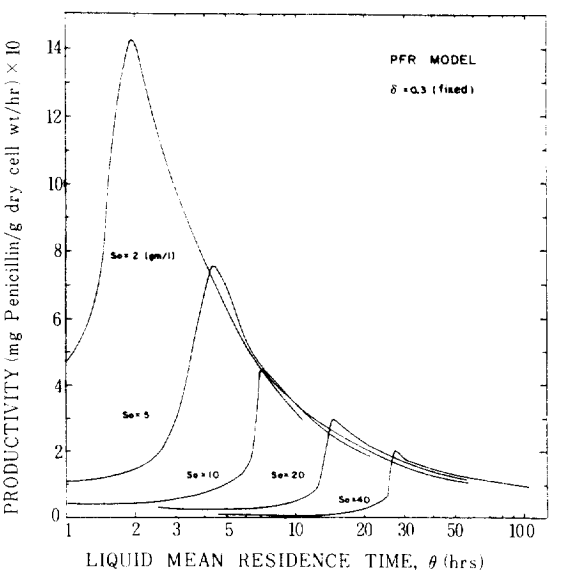

Fig. 8. Specific productivities of a PFR contacting pattern at various space times, $\delta = 0.3$.

creases. This is because the increase in maximum product concentration is much less than the increase in mean residence time which is required to achieve maximum product formation. Although more product is formed, it is done so at a slower overall rate. In other words, although the bulk substrate concentration is decreased by increasing θ, the mean residence time, the portion of the reactor occupied by a S_b favorable for pro-

duct formation is not increased as much as θ is, thus resulting in a lower overall productivity.

4.4. Effect of product decay

It should be noted that product decay effect has not been considered in the above discussions. Figs. 9 and 10 demonstrate the effect of this decay, employing the first-order decay rate used by Bajpai and Reuss. (11) Obviously, the product decay effect is most severe at high mean residence time and high inlet substrate concentration in a complete-mixed reactor. It significantly reduces the increase in outlet product concentration during the fermentor operation. However, comparing to a complete-mixed reactor, the product decay effect is less pronounced in a plug flow one at the same inlet substrate concentration and mean residence time. The characteristic profiles of bulk substrate concentration in the plug flow reactor, as discussed in the previous section, is responsible for this result. It emphasizes the fact that the product is formed only in the portion of the reactor toward the outlet such that increasing the feed mean residence time does not significantly increase the "residence time for product decay".

4.5. Comparison of complete-mixed and plug flow contacting patterns.

From the results shown in Fig. 5 through 8, it is clear that a complete-mixed contacting pattern is superior to a plug flow one for maximizing both the outlet product concentration and specific productivity of the system. This result is to be expected in light of the substrate inhibition effect on product synthesis by high substrate inhibition effect on product synthesis by high substrate concentrations at the reactor inlet of plug-flow configuration. In other words, the substrate inhibition (or carbon catabolite repression) effect is an important factor to be considered for selecting an appropriate contacting pattern in the three-phase fluidized-bed biofilm fermentor system for penicillin production. Inclusion of product decay effect during the fermentor operation (first order decay of produced penicillin to penicilloic acid, see Figs. 9 and 10) will slightly reduce the advantage of complete-mixed contacting pattern at long residence times, but the superiority over the plug-flow system is still quite appreciable. Consequently, to assure the complete-mixed contacting pattern in a fluidized-bed biofilm fermentor, choosing a reactor of small H/D ratio (height/diameter) and/or with a recycle stream is considered to be an important criterion for the design purposes. It should be noted, however, that the less sensitive effect of product decay can be a major advantage of plug flow contacting pattern when product decay is controlling the economy of the fermentor system.

CONCLUSION

From the steady-state analysis, it was found that a

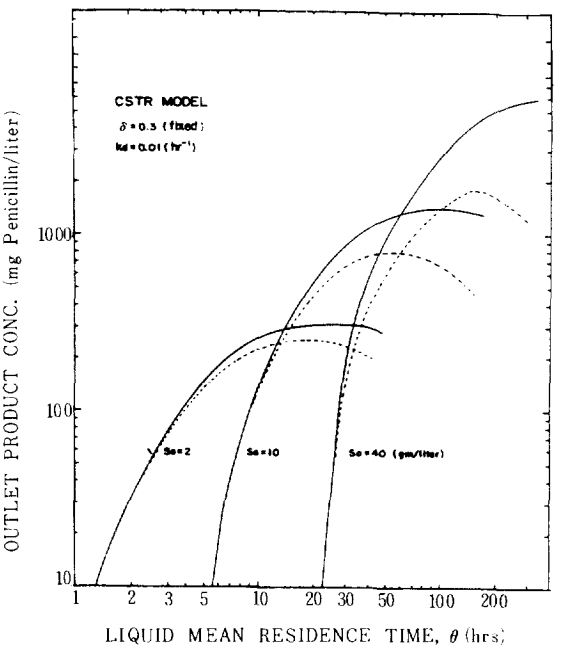

Fig. 9. Effect of product decay on the outlet product concentration in a CSTR contacting pattern: —without product decay, ···with product decay.

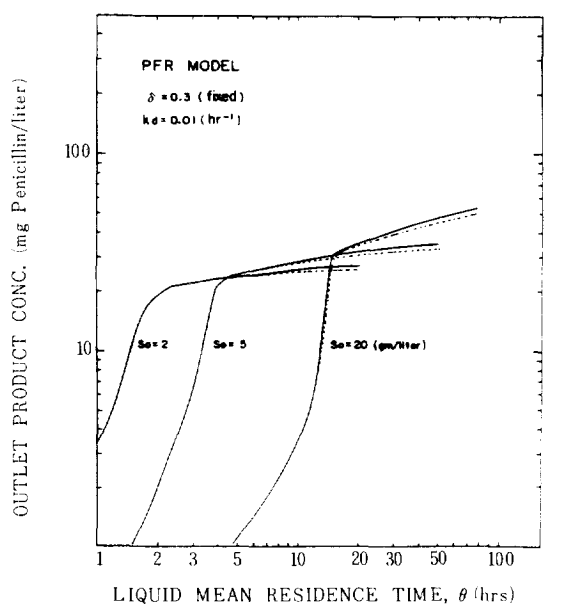

Fig. 10. Effect of product decay on the outlet product concentration in a PFR contacting pattern: —: without product decay, ··· with product decay.

complete-mixed contacting pattern gives a higher specific productivity and outlet product concentration than a plug flow pattern, mainly because that the effect of substrate inhibition on product formation is less pronounced in that configuration. Therefore, for a three-phase fluidized-bed biofilm fermentor, choosing reactors of small Height/Diameter ratios and/or with recycle streams is considered to be an important criterion for design purposes to assure the complete-mixed ocntacting pattern. It is also noted that some other characteristics of the fermentation system, such as product decay, can influence the criteria for selecting the contacting pattern. Although the complete-mixed contacting pattern is still superior to plug flow one with the first order product decay rate of kd = 0.01 (hr^{-1}) in this case of study, the latter configuration can be of choice for more severe decay effect during the fermentor operation since such an effect is much less pronounced in this case.

It is also found that the optimum biofilm thickness for steady-state operation is a function of the other operating variables, such as inlet substrate concentration, mean residence time, contacting patterns, etc. Thus the optimum thickness of biofilm should not be determined directly from the penetration depth of a limiting nutrient, but from information on the interactions between the reactor productivity and the operating variables, such as inlet substrate concentration, mean residence time and contacting pattern, etc.

NOMENCLATURE

a : effective oxygen mass transfer area per unit volume of liquid phase (cm^{-1})

Co : dissolved oxygen concentration (μmole O_2/cm^3)

D : effective diffusivities within biofilm (cm^2/hr)

H : Henry's law constant for oxygen (cm^3-atm/μmole O_2

k_d : first-order product decay constant (hr^{-1})

k_l : liquid side mass transfer coefficient between air bubble and liquid (cm/hr)

K_i : substrate inhibition constant (mg glucose/cm^3

K_{op} : Contois saturation constant for oxygen limitation of product formation (μmole O_2/mg dry cell wt)

K_{ox} : Contois saturation constant for oxygen limitation ob biomass production (μmole O_2/mg dry cell wt)

K_p : Monod saturation constant for substrate limitation of product formation (mg glucose/cm^3)

K_x : Contois saturation constant for substrate limitation ot biomass production (mg glucose/mg dry cell wt)

m_o : maintenance coefficient of oxygen (μmole O_2/mg dry cell wt/hr)

m_s : maintenance coefficient of substrate (mg glucose/mg drycell wt/hr)

N_p : total number of bioparticles in the reactor

P : penicillin concentration (mg penicillin/cm^3)

Po_2 : partial pressure of oxygen (atm)

Q : feed flow rate of liquid substrate (cm^3/hr)

r : radial coordinate, distance from the center of a bioparticle (cm)

R : gas law constant

R_f, R_o : radii of bioparticle with and without biofilm (cm)

R_{o2} : rate of oxygen consumption (μmole O_2/cm^3/hr)

R_p, R_s, R_x : rates of product formation, substrate consumption and biomass production ($mg/cm^3/hr$)

T : temperature of reactor system (°K)

U_p : maximum specific rate of product formation (mg penicillin/mg dry cell wt/hr)

U_x : maximum specific growth rate (hr^{-1})

V : volume of liquid-solid phase in the reactor (cm^3)

V_p : volume of bioparticle (cm^3)

X : biomass concentration in the biofilm (mg dry cell wt/cm^3)

Yp/o : yield coefficient of product on oxygen (mg penicillin/μmole O_2)

Yp/s : yield coefficient of product on substrate (mg penicillin/mg glucose)

Yx/o : yield coefficient of biomass on oxygen (mg dry cell wt/μmole O_2)

$Y_{x/s}$: yield coefficient of biomass on substrate (mg dry cell wt/mg glucose)

Greek Letters

δ : dimensionless biofilm thickness

ε : volume fraction occupied by liquid

θ : mean residence time of liquid substrate (hr)

ξ : dimensionless radial distance, r/R_o

Subscripts

b : indicates the conditions in bulk liquid phase

o : initial condition

in : inlet condition

REFERENCES

1. Kornegay, B.H., Andrews, J.F.: J. Water Poll. Control Fed., **40** (11), part 2, R460 (1968).
2. Jerris, J.S., Owens, R.W., Hickey, R.: J. Water Poll. Control. Fed., **49,** 816 (1977).
3. Atkinson, B.: Biochemical Reactors, Pion Press, London (1974).
4. Atkinson, B., Fowler, H.W.: Adv. Biochem. Eng. (T.K. Ghose, A. Fichter and N. Blakebrough, eds.), Springer-Verlag, New York, Vol. **3,** 221 (1974).
5. Atkinson, B., Knights, A.J.: Biotechnol. Bioeng., **17,** 1245 (1975).
6. Brifaud, J., Engasser, J.-M.: Biotechnol. Bioeng., **21,** 2093 (1979).
7. Constantinides, A., Spencer, J.L., Gaden, E.L. Jr.: Biotechnol. Bioeng., **12,** 803 (1970).
8. Calam, C.T., Ismail, B. A-K.: J. Chem. Tech. Biotechnol., **30,** 249 (1980).
9. Heijnen, I.J., Roels, J.A., Stauthamer, A.H.: Biotechnol. Bioeng., **21,** 2175 (1979).
10. Fisherman, V.M., Biryukov, V.V.: Biotechnol. Bioeng. Symp., No. 4, 647 (1974).
11. Bajpai, R.K., Reuss, M.: J. Chem. Tech. Biotechnol., **30,** 332 (1980).
12. Ryu, D.Y., Humphrey, A.E.: J. Ferment. Technol., **50** (6), 424 (1972).
13. Giona, A.R., Marrelli, L., Toro, L.: Biotechnol. Bioeng., **18,** 1249 (1976).
14. Bajpai, R.K., Reuss, M.: Biotechnol. Bioeng., **23,** 717 (1981).
15. Merchuk, J.C., Stein, Y., Mateles, R.I.: Biotechnol. Bioeng., **22,** 1189 (1980).
16. Rittmann, B.E.: Biotechnol. Bioeng., **24,** 1341 (1982).
17. Andrews, G.F.: Biotechnol. Bioeng., **24,** 2013 (1982).
18. Van Suijdam, J.C., Hols, H., Kossen, N.W.F.: Biotechnol. Bioeng., **24,** 177 (1982).
19. Froment, G.F., Bischoff, K.B.: Chemical Reactor Analysis and Design, John Wiley & Sons, New York (1979).
20. Alvarez-Guenka, M., Nerengerg, M.A.: Can. J. Chem. Eng., **59,** 739 (1981).
21. Deckwer, W.D., Nguen-Tien, K., Schumpe, A., Serpemen, Y.: Biotechnol. Bioeng., **24,** 461 (1982).
22. Park, Y.H., Davis, M.E., Wallis, D.A.: Biotechnol. Bioeng. accepted for publication (1984).
23. Ascher, U., Christiansen, J., Russells, R.D.: ACM Trans. math. Softw., **7,** 209 (1981).
24. De Boor, C.: J. Approx. Theory, **6** (1), 50 (1972).